Talanta 82 (2010) 340–347

Contents lists available at ScienceDirect

Talanta

journal homepage: www.elsevier.com/locate/talanta

Electrode modified with a composite film of ZnO nanorods and Ag nanoparticles as a sensor for hydrogen peroxide

Chia-Yu Lin[a], Yi-Hsuan Lai[a,b], A. Balamurugan[a], R. Vittal[a], Chii-Wann Lin[b,c], Kuo-Chuan Ho[a,d,*]

[a] Department of Chemical Engineering, National Taiwan University, Taipei 10617, Taiwan
[b] Institute of Biomedical Engineering, National Taiwan University, Taipei 10617, Taiwan
[c] Institute of Electrical Engineering, National Taiwan University, Taipei 10617, Taiwan
[d] Institute of Polymer Science and Engineering, National Taiwan University, Taipei 10617, Taiwan

ARTICLE INFO

Article history:
Received 22 January 2010
Accepted 22 April 2010
Available online 29 April 2010

Keywords:
Amperometric detection
Hydrogen peroxide sensor
Modified electrode
Silver nanoparticles
Zinc oxide nanorods

ABSTRACT

A conducting fluorine-doped tin oxide (FTO) electrode, first modified with zinc oxide nanorods (ZnONRs) and subsequently attached with photosynthesized silver nanoparticles (AgNPs), designated as AgNPs/ZnONRs/FTO electrode, was used as an amperometric sensor for the determination of hydrogen peroxide. The first layer (ZnONRs) was obtained by chemical bath deposition (CBD), and was utilized simultaneously as the catalyst for the photoreduction of Ag ions under UV irradiation and as the matrix for the immobilization of AgNPs. The aspect ratio of ZnONRs to be deposited was optimized by controlling the number of their CBDs to render enough surface area for Ag deposition, and the amount of AgNPs to be attached was controlled by adjusting the UV-irradiation time. The immobilized AgNPs showed excellent electrocatalytic response to the reduction of hydrogen peroxide. The resultant amperometric sensor showed 10-fold enhanced sensitivity for the detection of H_2O_2, compared to that without AgNPs, i.e., only with a layer of ZnONRs. Amperometric determination of H_2O_2 at −0.55 V gave a limit of detection of 0.9 μM (S/N = 3) and a sensitivity of 152.1 mA M^{-1} cm^{-2} up to 0.983 mM, with a response time (steady-state, t_{95}) of 30–40 s. The selectivity of the sensor was investigated against ascorbic acid (AA) and uric acid (UA). Energy dispersive X-ray (EDX) analysis, transmission electron microscopic (TEM) image, X-ray diffraction (XRD) patterns, cyclic voltammetry (CV), and scanning electron microscopic (SEM) images were utilized to characterize the modified electrode. Sensing properties of the modified electrode were studied both by CV and amperometric analysis.

1. Introduction

Research on the quantitative detection of hydrogen peroxide (H_2O_2) received considerable attention, because H_2O_2 is widely used as an oxidizing agent in chemical and food industries [1]. It is an essential mediator in food, pharmaceutical, clinical, and environmental analysis. Besides, H_2O_2 is produced during some chemical and enzymatic processes [2,3]; its detection can be used as an indicator for the progress of such processes. Several techniques, including spectrophotometry, chemiluminescence, fluorometry, have been developed for the determination of H_2O_2 [4–7]; some of them involve time-consuming and tedious procedures. Electrochemical technique is an appropriated alternative or a complementary choice, with respect to the mentioned techniques; it has been proved to be an inexpensive and effective way for quantitative determination owing to its intrinsic sensitivity, fast analysis, high selectivity and simplicity. H_2O_2 can be detected anodically at a platinum electrode at around +0.7 V vs. SCE; it can also be detected cathodically at a copper electrode at −0.25 V vs. SCE [1].

The presence of nanoparticles in electrochemical sensors can decrease the over-potentials of many analytes that occur at unmodified electrodes. Metal nanoparticles (NPs), such as PtNPs [7], AgNPs [8], AuNPs [9], and PdNPs [10] have been proposed as electrocatalysts for sensing H_2O_2, owing to their excellent conductivity, extraordinary electrocatalytic property, and larger specific surface area. Among these materials, silver nanoparticles (AgNPs) show excellent electrocatalytic activity for H_2O_2 [11,12]. Recent studies [13,14] indicate that the size distribution of AgNPs plays an important role in their electrocatalytic activity for H_2O_2.

Photochemical reduction of some metal nanoparticles, e.g., those of Ag^+, Cu^{2+}, Cd^{2+}, Pt^{4+}, Au^{3+}, through semiconducting materials assumes importance, because of the associated mild synthetic conditions and because that the amount and size of metal NPs

* Corresponding author at: Department of Chemical Engineering, National Taiwan University, No. 1, Sec. 4, Roosevelt Rd., Taipei 10617, Taiwan. Tel.: +886 2 2366 0739; fax: +886 2 2362 3040.
E-mail address: kcho@ntu.edu.tw (K.-C. Ho).

0039-9140/$ – see front matter © 2010 Elsevier B.V. All rights reserved.
doi:10.1016/j.talanta.2010.04.047

can be controlled by varying the conditions of the photochemical reduction process [15–18]. Among the metal/semiconductor composites, Ag/ZnO is an important combination for the reduction of Ag^+, since the consequent quantum yield of AgNPs is usually high [19], and the resulting AgNPs find potential applications for chemical sensors [20], antibacterial agents [21], photocatalysts [22], etc. Koga et al. have recently reported *in situ* synthesis of AgNPs on zinc oxide whiskers incorporated in a paper matrix [21]. Cui et al. have electrodeposited AgNPs on three-dimensional DNA networks that were directly dropped on the surface of glassy carbon electrode (GCE); the composite was used as a sensor for H_2O_2 [14].

This study reports the preparation of a modified electrode and its application as a sensor for the amperometric detection of H_2O_2 using fluorine-doped tin oxide (FTO) substrate, modified with a composite film of zinc oxide nanorods (ZnONRs) and AgNPs, designated as AgNPs/ZnONRs/FTO electrode. ZnONRs were directly grown onto the FTO substrate by chemical bath deposition (CBD), and AgNPs were subsequently attached to ZnONRs by a photoreduction method, under UV irradiation (λ = 365 nm). The aspect ratio of ZnONRs to be deposited was optimized by controlling the number of CBD, and the amount of AgNPs to be attached was controlled by adjusting the UV-irradiation time. Although there have been reports on the photosynthesis of AgNPs onto ZnO nanoparticles [15–18], these reports were restricted to the preparation and characterization of the nanoparticles, but not focused on their sensor applications. The application of this modified electrode as an electrochemical sensor for the detection of H_2O_2 is a novel aspect of this research.

2. Experimental

2.1. Chemicals

Zinc nitrate (99%), hexamethylenetetramine (HMT, 99.5%), and silver nitrate (99.9%) were purchased from Riedel-de Haën, and used as received. 50 mM of H_2O_2 sample solution was prepared before each experiment by direct dilution of H_2O_2 (35%, Sigma–Aldrich) in deionized water (DIW) and deaerated by purging it with nitrogen for 20 min. Other chemicals were of analytical grade and used without further purification. DIW was used throughout the work.

2.2. Apparatus

Cyclic voltammetry (CV) and amperometric experiments were performed at a CHI 440 electrochemical workstation (CH Instruments, Inc., USA) using a conventional three-electrode system. AgNPs/ZnONRs/FTO electrode was used as the working electrode. A Pt foil (4.0 cm × 1.0 cm) and Ag/AgCl/saturated KCl (homemade) served as the counter and reference electrode, respectively. All electrochemical experiments were performed at room temperature and all the potentials are reported against the Ag/AgCl/sat'd KCl reference electrode.

The nanostructure of AgNPs/ZnONRs composite was obtained by using scanning electron microscope (SEM, Nova NanoSEM 230); elemental analysis was made using the same SEM, with an additional provision of x-sight light element energy dispersive X-ray (EDX) spectrometer (Oxford Instruments 6560 INCA). Transmission electron microscopy (TEM, Hitachi H-7100, Japan) was also used to obtain the image of AgNPs/ZnONRs composite structure. The presence of ZnO and Ag in the composite film of AgNPs/ZnONRs was verified by X-ray diffraction patterns (XRD, X-Pert, the Netherlands) with Cu Kα radiation.

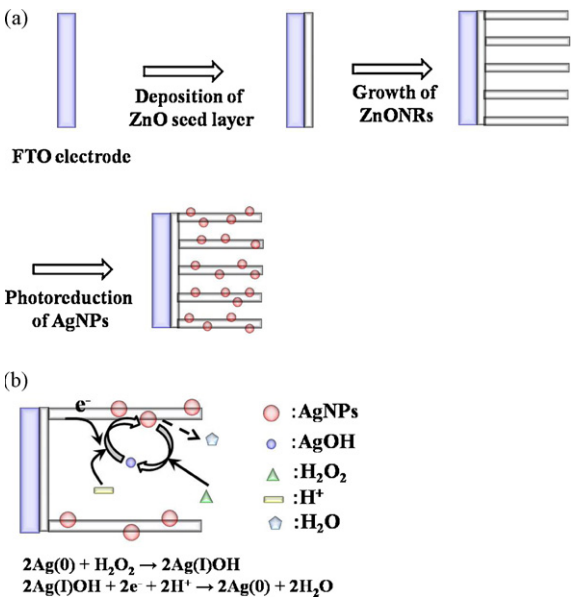

Scheme 1. (a) Flow sheet for the preparation of AgNPs/ZnONRs/FTO modified electrode. (b) The reactions occurring at the surface of the modified electrode for the detection of hydrogen peroxide.

2.3. Preparation of AgNPs/ZnONRs-modified electrode

The flow sheet for the preparation of AgNPs/ZnONRs-modified electrode is shown in Scheme 1. Before the formation of ZnONRs, a thin film of ZnO was deposited onto the FTO substrate, by spin-coating 0.1 M of zinc acetate solution and annealing the substrate at 200 °C for 30 min; this thin film of ZnO served as the seeding layer for ZnONRs. ZnONRs were then allowed to grow on the ZnO-seeded FTO glass substrate (Solaronix SA, 15 Ω/□, with a geometric area of 1.5 cm^2) by the CBD, by namely suspending the ZnO-seeded substrate upside down in a glass bottle filled with an equimolar (20 mM) aqueous solution of zinc nitrate and HMT. The thus prepared electrode is designated as ZnONRs/FTO. During the growth, the glass bottle was sealed and heated in a laboratory oven at 90 °C for 4 h ($ZnONRs_{G1}$/FTO). To obtain ZnONRs with a high aspect ratio, the deposition was repeated in fresh precursor solutions for 2, 3 and 4 growth cycles, and the electrodes deposited with 2, 3, and 4 growth cycles of ZnONRs were designated as $ZnONRs_{G2}$/FTO, $ZnONRs_{G3}$/FTO, and $ZnONRs_{G4}$/FTO, respectively. At the end of each growth cycle, the substrate was removed from the solution and rinsed immediately with DIW to remove any residual salt from the surface, and dried in air at room temperature.

After the formation of ZnONRs, AgNPs were photochemically deposited on the ZnONRs by suspending the ZnONRs/FTO electrode upside down in a glass bottle with 0.5 mM of silver nitrate aqueous solution containing a mixer. During the loading of AgNPs, the bottle was placed inside a photochemical reactor (Panchum Scientific Corp., Taiwan) and was irradiated with UV light (power density: 0.14 W cm^{-2}; main wavelength: 365 nm) for a specific period of time, under forced air convection. After the deposition of AgNPs, the electrode was removed from the solution, immediately rinsed with DIW to remove any residual salt from the surface, and dried in air at room temperature.

2.4. Amperometric detection of H_2O_2

For the detection of H_2O_2 with amperometry at constant potential by using AgNPs/ZnONRs/FTO electrode as the sensor, a suitable sensing potential in the limiting current plateau region between 0 and −0.7 V was determined by applying linear sweep voltamme-

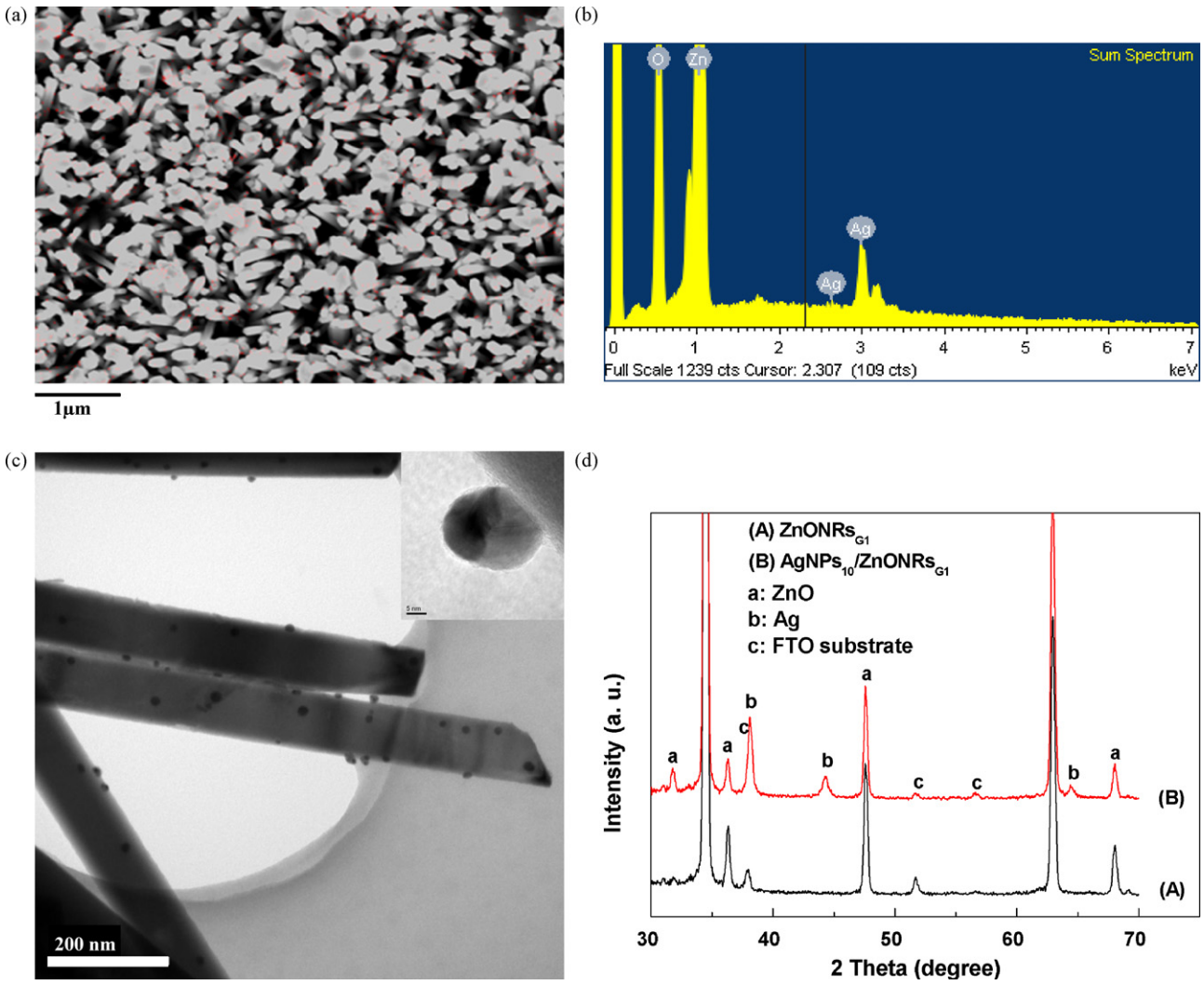

Fig. 1. (a) EDX mapping image of the composite film of AgNPs/ZnONRs. AgNPs are marked with red spots; (b) EDX elemental analysis of AgNPs deposited onto ZnONRs; (c) TEM image of ZnONRs adhered with AgNPs. The inset is the HRTEM image of a ZnONR attached with a tiny AgNP; (d) XRD patterns of ZnONRs/FTO and AgNPs/ZnONRs/FTO. The number of cycle and irradiation time for the growth of ZnONRs and AgNPs were kept at 1 and 10 min, respectively. (For interpretation of the references to color in this figure legend, the reader is referred to the web version of the article.)

try in a solution containing deaerated 0.1 M PBS (pH 7) and 0.5 mM H_2O_2 (not shown). Considering the sensitivity and the steadiness of AgNPs/ZnONRs/FTO electrode, the sensing potential was chosen to be −0.55 V. Current densities in the concentration range of 8 μM to 1 mM were collected, and pertaining calibration curve was constructed for the detection of H_2O_2.

3. Results and discussion

3.1. Characterization of AgNPs/ZnONRs

When the silver ions in the silver nitrate solution receive excited electrons, from ZnONRs, AgNPs are photochemically deposited onto the ZnONRs/FTO electrode under UV irradiation [18]. The presence of AgNPs on the ZnONRs could be verified by EDX analyses (Fig. 1a and b), TEM image (Fig. 1c), and through XRD-patterns (Fig. 1d). Fig. 1a–d also shows the dominant presence of ZnONRs. AgNPs are marked in Fig. 1a with red spots. The number of cycle and irradiation time for the growth of ZnONRs and AgNPs were 1 and 10 min, respectively; they are correspondingly designated as ZnONRs$_{G1}$ and AgNPs$_{10}$. The distribution of AgNPs is quite uniform (Fig. 1a); the sizes of AgNPs range from 10 to 20 nm, as judged by the TEM image in Fig. 1c; the inset is the HRTEM image of a ZnONR attached with a tiny AgNP. XRD peaks in Fig. 1d confirm the crystal structure of the component elements in the composite film of AgNPs/ZnONRs. The XRD pattern shows typical peaks of crystalline ZnONRs and two peaks at $2\theta = 38^\circ$ and 44°, corresponding to the characteristic (1 1 1) and (2 0 0) reflections of crystalline Ag.

3.2. Sensing behavior of AgNPs/ZnONRs for H_2O_2

The electrocatalytic behavior of *AgNPs/ZnONRs*-modified electrode towards the electrochemical reduction of H_2O_2 was studied using cyclic voltammetry. Fig. 2a and b shows, respectively the cyclic voltammetric responses of ZnONRs$_{G1}$/FTO and AgNPs$_{10}$/ZnONRs$_{G1}$/FTO electrodes in 0.1 M phosphate buffer solution (PBS, pH 7) for various concentrations of H_2O_2 ranging from 0, 0.5, 1.0, and 1.5 mM. The CVs both in Fig. 2a and b represent the catalytic currents due to the reduction of H_2O_2. In the blank phosphate buffer, no faradic current appears (Fig. 2a and b). A maximum reduction current density of 30 μA/cm^2 can be seen with the addition of 1.5 mM of H_2O_2 in the case of ZnONRs$_{G1}$/FTO electrode (Fig. 2a), while a reduction current density of about 300 μA/cm^2 can be seen with AgNPs$_{10}$/ZnONRs$_{G1}$/FTO electrode for the same addition of H_2O_2 (Fig. 2b). The immobilized AgNPs exhibited excellent electrocatalytic response for the reduction of hydrogen peroxide.

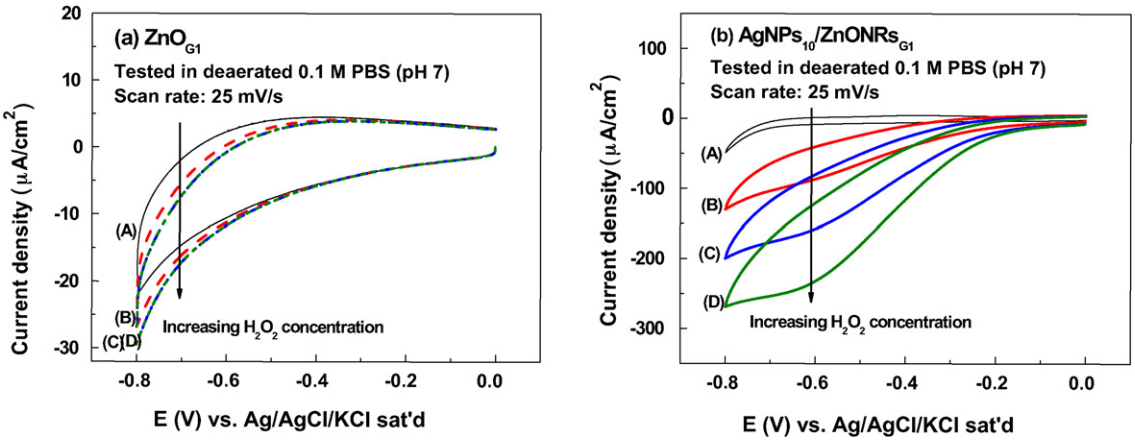

Fig. 2. Cyclic voltammetric responses of (a) ZnONRs$_{G1}$/FTO electrode and (b) AgNPs$_{10}$/ZnONRs$_{G1}$/FTO electrode in deaerated 0.1 M PBS (pH 7) containing various concentrations of H_2O_2 ranging from (A) 0, (B) 0.5, (C) 1.0, and (D) 1.5 mM, at a scan rate of 25 mV/s.

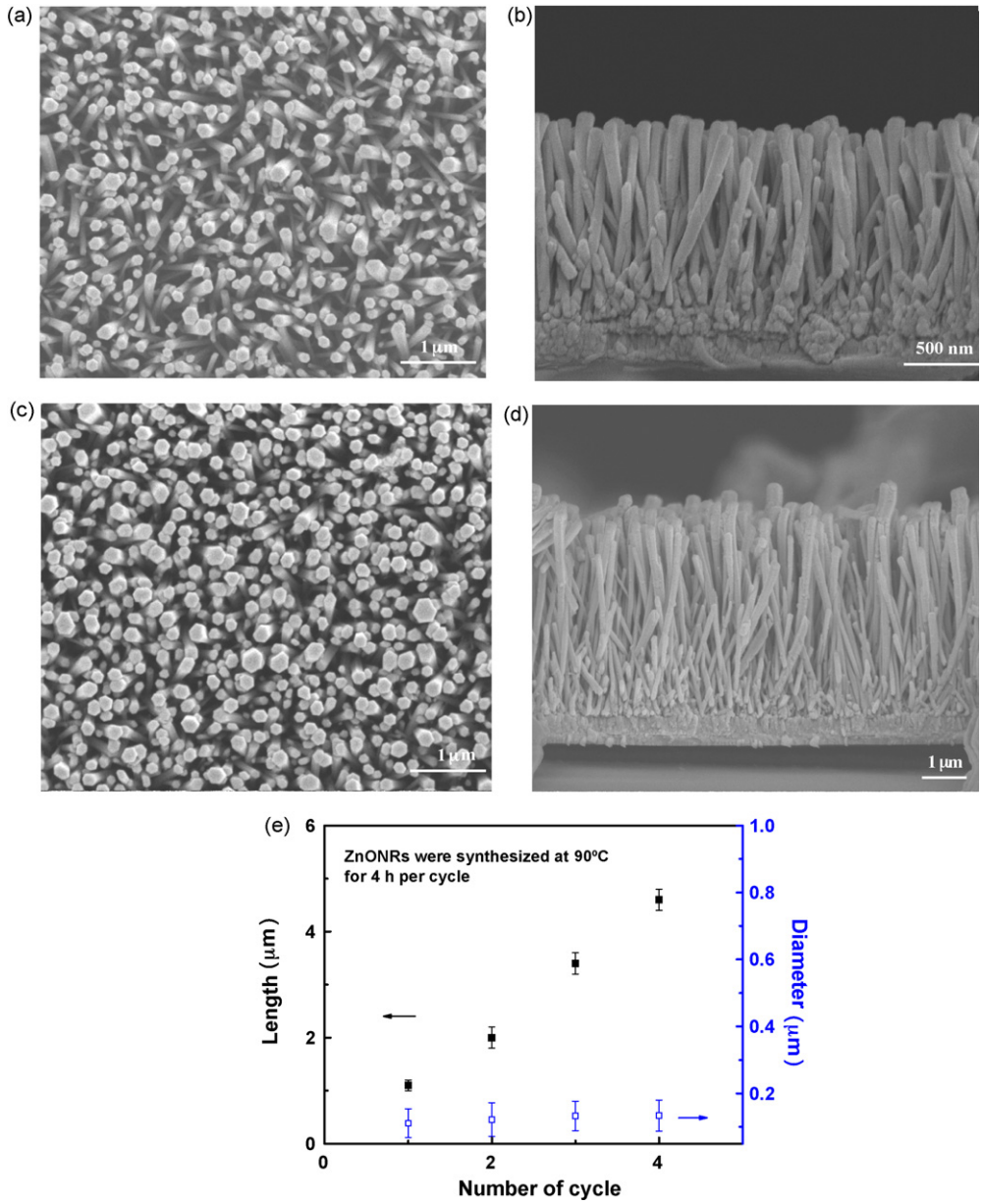

Fig. 3. The top and cross-sectional SEM views of (a, b) ZnONRs$_{G2}$/FTO and (c, d) ZnONRs$_{G4}$/FTO; (e) variation of length (closed squares) and diameter (open squares) of the ZnONRs with the number of growth cycles.

Table 1
Length, diameter, and corresponding aspect ratio of the ZnONRs grown at different growth cycles.

	Number of growth cycle for ZnONRs preparation			
	1 (G1)	2 (G2)	3 (G3)	4 (G4)
Length, L (μm)	1.1	2	3.4	4.6
Diameter, D (nm)	109	122	133	134
Aspect ratio (L/D)	10.1	16.4	25.6	34.3

The reduction currents of H_2O_2 with the AgNPs/ZnONRs/FTO electrode are 10-fold higher than those with the ZnONRs/FTO electrode, clearly revealing the remarkable improvement in the electrocatalytic ability of ZnONRs film with the attachment of AgNPs; thus the presence of AgNPs is responsible for the greatly enhanced performance of the sensor. The enhanced catalytic current of the sensor can be mainly attributed to the large number of small AgNPs on the electrode and their nano-scale dimensions [14,23–25]. Namely, the ZnONRs/AgNPs nano-composite could provide a three-dimensional network, thereby increasing the surface area of the AgNPs/ZnONRs/FTO electrode and its catalytic ability by 10-fold for the detection of H_2O_2, with reference to the catalytic ability of mere ZnONRs/FTO electrode. In other words, the nano-size AgNPs created more active sites on the ZnONRs/FTO surface in the nanoparticle-assisted catalysis. Intending to optimize the sensor response within our experimental conditions, the deposited amount of AgNPs was increased by increasing the surface area of ZnONRs-matrix and the duration of UV irradiation. The surface area of ZnONRs, controlled by the aspect ratio, could be increased by increasing the number of growth cycles. Fig. 3a and b shows the top and cross-sectional SEM views of $ZnONRs_{G2}$/FTO, and Fig. 3c and d such pictures of $ZnONRs_{G4}$/FTO. Fig. 3e shows the variation of length (closed squares) and diameter (open squares) of the ZnONRs with the number of growth cycle. It can be seen in Fig. 3e that the average length of ZnONRs increases considerably with the number of growth cycles from 1 to 4; Fig. 3a and c also reveal that the diameter of the ZnONRs hardly experiencing any change. Table 1 gives the values of length, diameter, and corresponding aspect ratio for the ZnONRs grown at different growth cycles. The longitudinal growth of the ZnONRs, with the increase of growth cycle from 1 to 4, has resulted in the increase in the aspect ratio of ZnONRs from 10.1 to 34.3 (Fig. 3b and d and Table 1), and thereby increasing their surface area.

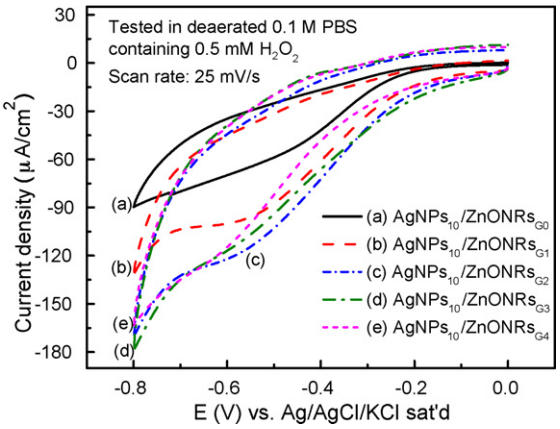

Fig. 4. Cyclic voltammetric responses of AgNPs/ZnONRs/FTO electrodes at a scan rate of 25 mV/s, in which the ZnONRs were obtained using various numbers of growth cycle, and the AgNPs were obtained using an irradiation time of 10 min; the electrolyte contained 0.1 M PBS (pH 7) and 0.5 mM of H_2O_2.

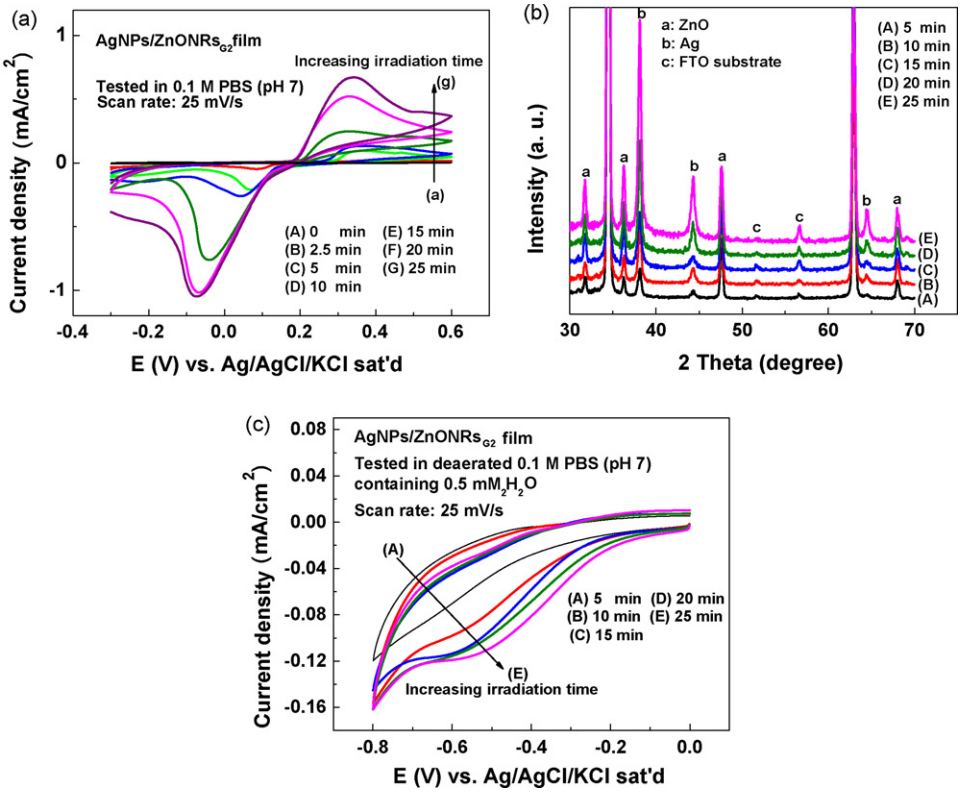

Fig. 5. (a) Cyclic voltammetric responses of FTO electrodes modified with ZnONRs for 2 cycles, and further deposited with AgNPs, using various irradiation times of UV light, in 0.1 M PBS (pH 7) at a scan rate of 25 mV/s; (b) XRD patterns of AgNPs/ZnONRs/FTO electrodes, prepared with various irradiation times of AgNPs deposition; (c) Cyclic voltammetric responses of AgNPs/$ZnONRs_{G2}$/FTO electrodes, prepared with various irradiation times of AgNPs loading, in deaerated 0.1 M PBS (pH 7) containing 0.5 mM of H_2O_2 at a scan rate of 25 mV/s.

Table 2
Estimated crystal sizes of AgNPs, photochemically deposited onto the ZnONRs after irradiating the ZnONRs/FTO electrodes for various times.

Irradiation time (min)	Crystal size (nm)
5	13.4
10	14.1
15	14.1
20	14.3
25	15.9

Fig. 4 depicts the cyclic voltammetric responses of AgNPs/ZnONRs/FTO electrodes, in which the ZnONRs were obtained using various numbers of growth cycle, and the AgNPs were obtained using an irradiation time of 10 min; the electrolyte contained 0.1 M PBS (pH 7) and 0.5 mM of H_2O_2. Note that $ZnONR_{G0}$/FTO stands for an FTO electrode with only a seeding layer of ZnO. It can be seen in Fig. 4 that the cathodic peak current density increases with increasing growth cycle up to 2. However, the cathodic peak current density remains almost the same as the growth cycle number exceeds 2. Although the surface area, controlled by the aspect ratio, increases with increasing number of ZnO growth cycle (Table 1), the distance of diffusion path for the electroactive species also increases as a consequence. Thus, an optimum aspect ratio of ZnONRs is to be chosen for the better performance of the sensor. Careful observation reveals that the peak potential shows a slight shift to the negative side, as the number of growth cycle is greater than 2; this can be attributed to the increase in the distance of diffusion path for the electroactive species to reach the electrode surface for electron transfer. Therefore, we selected 2 cycles as the optimal number of growth cycle for further experiments.

Fig. 5a shows the cyclic voltammetric responses of FTO electrodes modified with ZnONRs for 2 cycles, and further deposited with AgNPs, using various irradiation times of UV light, in 0.1 M PBS (pH 7) at a scan rate of 25 mV/s. It can be seen that the redox peak current density of AgNPs/ZnONRs/FTO electrodes increases with the irradiation time from 0 to 25 min, suggesting that the deposited amount of AgNPs increases with the irradiation time. Fig. 5b shows the XRD patterns of AgNPs/ZnONRs/FTO electrodes with various irradiation times for the deposition of AgNPs. The increase in peak heights with increase in irradiation time reveals the increase in deposited amount of AgNPs. Besides, the grain size of AgNPs also increases as the irradiation time increases (Table 2). Grain size was obtained using Scherrer's formula as shown below:

$$d = \frac{\lambda}{B\cos\theta} \quad (1)$$

where λ and B are the wavelength of X-ray and the full-width at half maximum intensity, respectively. Fig. 5c shows cyclic voltammetric responses of $AgNPs/ZnONRs_{G2}$/FTO electrodes, prepared with various irradiation times of AgNPs deposition, in deaerated 0.1 M PBS (pH 7) containing 0.5 mM of H_2O_2 at a scan rate of 25 mV/s. An increase in the peak current density for H_2O_2 reduction is noticed, with the increase in the irradiation time. The increase in peak current density implies an increase in the deposited amount of AgNPs. This also suggests that higher amount of AgNPs can render higher catalytic ability to the modified electrode. It is clear in Fig. 5c that a maximum reduction current density can be obtained with 25 min of irradiation time. Therefore, we selected 25 min as the optimal irradiation time for the deposition of AgNPs in further experiments.

3.3. Cyclic voltammetric detection of H_2O_2

Fig. 6a depicts the cyclic voltammetric responses of a $AgNPs_{25}/ZnONRs_{G2}$/FTO electrode in 0.1 M PBS (pH 7) containing 1.5 mM H_2O_2 at various scan rates ranging from 3.125 to 200 mV s^{-1}. The number of growth cycle for the deposition of ZnONRs and the irradiation time for the attachment of AgNPs were 2 and 25 min, respectively. A linear relationship can be seen between the peak current density (J_{pa}) and the square root of scan rate ($\nu^{1/2}$) in Fig. 6b (correlation coefficient, $R^2 = 0.995$), which suggests that the rate of electrochemical reaction is rather fast and the electrode process is controlled by the diffusion of the analyte from solution to the electrode surface. In addition, the number of electrons transferred in the rate-determining step (n_α) and the electron transfer coefficient (α) can be obtained according to Eq. (2) [26]:

$$\alpha n_\alpha = \frac{47.7\,\text{mV}}{|E_p - E_{p/2}|} \quad (2)$$

where E_p and $E_{p/2}$ are the peak potential and the potential at the half maximum peak current, respectively. The value of αn_α was estimated to be 0.435, suggesting that the rate-determining step involves one electron transfer, because the value of α ranges between 0.3 and 0.7 [26].

Scheme 1 shows the reactions occurring at the surface of the modified electrode for the detection of hydrogen peroxide. A possible mechanism for the reduction of H_2O_2 at AgNPs/ZnONRs/FTO electrode is proposed. First, H_2O_2 reacts with AgNPs on ZnO to give argentous hydroxide [11], which subsequently gets electroreduced to renewed AgNPs on Ag/ZnO (see Eqs. (3) and (4)).

$$2Ag(0) + H_2O_2 \rightarrow 2Ag(I)OH \quad (3)$$

$$2Ag(I)OH + 2e^- + 2H^+ \rightarrow 2Ag(0) + 2H_2O \quad (4)$$

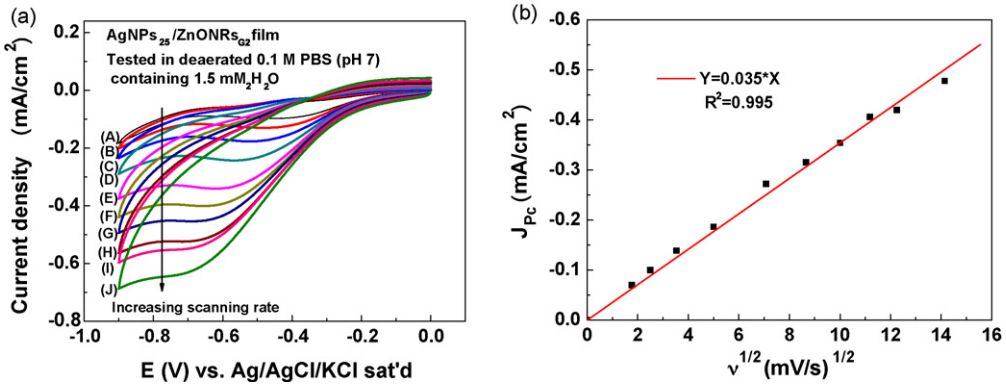

Fig. 6. (a) Cyclic voltammograms of $AgNPs/ZnONRs_{G2}$/FTO electrode (growth cycle 2, irradiation time: 25 min) in 0.1 M PBS (pH 7) solution containing 1.5 mM H_2O_2 at various scan rates of (A) 3.125, (B) 6.25, (C) 12.5, (D) 25, (E) 50, (F) 75, (G) 100, (H) 125, (I) 150, and (J) 200 mV s^{-1}; (b) Relationship between the peak current density (J_{pa}) and the square root of scan rate ($\nu^{1/2}$).

Table 3
A partial list of literature on electrochemical H_2O_2 sensing, using Ag modified electrodes.

Type of the electrode	Performance			Ref.
	Sens.[a] ($mA\,M^{-1}\,cm^{-2}$)	LOD (μM)	Linear range (mM)	
PEDOT[a]/AgNPs/GCE[b]	–	7	–	[8]
AgNPs/PVA[c]/Pt	4090	1.0	0.04–6	[11]
Ag microspheres/GCE[b]	–	1.2	0.25–2	[12]
AgNPs/collagen/GCE[b]	–	0.7	0.005–40.6	[13]
AgNPs/DNA/GCE[b]	–	1.7	0.004–16	[14]
AgNPs/DNA/GCE[b]	773	0.6	0.002–2.5	[23]
AgNPs/GCE[b]	2414	2	–	[24]
AgNPs/SBA-15/GCE[b]	–	12	0.049–970	[27]
Roughed Ag electrode	24.8	6	0.01–22.5	[28]
AgNPs/ZnONRs/FTO	152.1	0.9	0.008–0.983	This work

[a] Sensitivity.
[b] Poly(3,4-ethyldioxythiophene).
[c] Glassy carbon electrode.
[d] Polyvinyl alcohol.

3.4. Amperometric detection of H_2O_2 and the pertinent calibration curve

Fig. 7 shows a typical chronoamperometric response, i.e., a current–time plot of AgNPs/ZnONRs$_{G2}$/FTO electrode on successive droppings of the H_2O_2 solution of different concentrations into 0.1 M PBS solution (pH 7), at an applied potential of −0.55 V vs. Ag/AgCl/sat'd KCl. The number of growth cycle for the deposition of ZnONRs and the irradiation time for the loading of AgNPs were kept at 2 and 25 min, respectively. The calibration curve for H_2O_2 was constructed by measuring the changes in current with each addition of H_2O_2 at a specific concentration, and is shown in the inset of Fig. 7. It can be seen from the calibration curve that the cathodic current density increases linearly with the increase of concentration of H_2O_2 (correlation coefficient, $R^2 = 0.998$), which permits reliable quantification of the content of H_2O_2 in a sample. Besides, from the slope of the inset, the sensitivity of the AgNPs$_{25}$/ZnONRs$_{G2}$/FTO electrode was determined to be 152.1 $mA\,cm^{-2}\,M^{-1}$. The response time was estimated from the amperometric response curve (Fig. 7) by enlarging a small segment of it and was found to be 30–40 s. Since the electrochemical detection process was diffusion-limited, the relatively long diffusion length, resulted from the thick nanocomposite film, leads to this moderately slow sensor response. The limit of detection (LOD), based on signal-to-noise ratio of 3, for AgNPs$_{25}$/ZnONRs$_{G2}$/FTO electrode was also estimated from the calibration curve to be 0.9 μM. The reproducibility of the proposed sensor, evaluated in terms of the relative standard deviation ($n = 3$), was determined to be 4.4% (data not shown). Table 3 shows a partial list of literature on the amperometric detection of H_2O_2, using Ag modified electrodes. It can be seen in the table that the LOD for the AgNPs$_{25}$/ZnONRs$_{G2}$/FTO electrode in this study is comparable with or lower than those obtained with most of the other Ag modified electrodes.

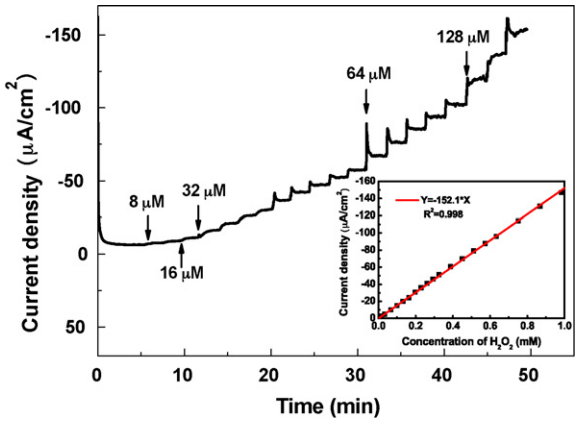

Fig. 7. Amperometric response of AgNPs/ZnONRs$_{G2}$/FTO electrode (growth cycle: 2, irradiation: 25 min) for various concentrations of H_2O_2 in 0.1 M PBS solution (pH 7) at an applied potential of −0.55 V vs. Ag/AgCl/sat'd KCl. Inset: the corresponding calibration curve for H_2O_2.

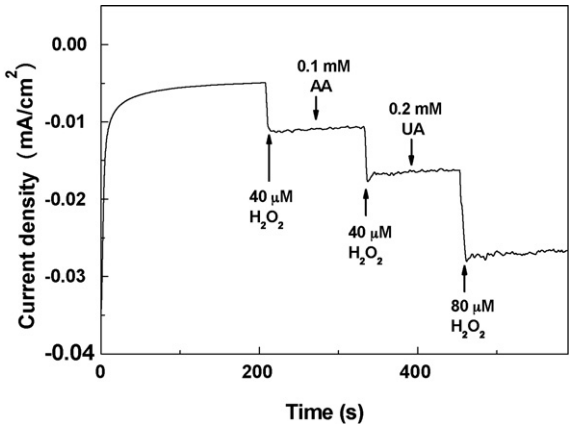

Fig. 8. Amperometric response of AgNPs/ZnONRs/FTO electrode (growth cycle: 2, irradiation: 25 min) for various concentrations of H_2O_2, AA, and UA in a deaerated solution containing 0.1 M PBS (pH 7) at an applied potential of −0.55 V vs. Ag/AgCl/sat'd KCl.

The selectivity of the sensor was also evaluated against ascorbic acid (AA) and uric acid (UA); AA and UA are commonly present in the physiological samples and they pose interference in the analysis of H_2O_2 in such samples. Fig. 8 shows amperometric response of AgNPs/ZnONRs/FTO electrode for H_2O_2, AA, and UA in a deaerated solution of 0.1 M PBS (pH 7) at an applied potential of −0.55 V. The number of growth cycle for the deposition of ZnONRs and the irradiation time for the deposition of AgNPs were kept at 2 and 25 min, respectively. As shown in Fig. 8, there is obvious current response to the addition of 40 μM H_2O_2. On the contrary, no current response is observed to the additions of 0.1 mM AA and 0.2 mM UA in the same sample, indicating that AA and UA have no interference in the determination of 40 μM H_2O_2.

4. Conclusions

AgNPs/ZnONRs/FTO modified electrode was prepared by successfully depositing AgNPs (10–20 nm) by UV-light irradiation on ZnONRs that were initially deposited by CBD on FTO electrode, and its application for amperometric detection of H_2O_2 was investigated. The catalytic ability of ZnNRs covered FTO electrode for H_2O_2 detection was enhanced by 10-fold with further modifica-

tion of the ZnNRs/FTO electrode with AgNPs. The presence of AgNPs is responsible for the greatly enhanced performance of the sensor. ZnONRs could be grown on FTO electrode only longitudinally with the increase of the number of growth cycle (number of CBDs). Sensitivity of the modified electrode showed an increase with the increase of irradiation time, i.e., with the corresponding increase of deposited amount of AgNPs. It was shown that the electroreduction of H_2O_2 is a diffusion-controlled process catalyzed by AgNPs. A linear relationship could be obtained between the current density and the concentration of H_2O_2 up to 1 mM, suggesting successful construction of a sensor for the detection of H_2O_2 for this concentration range. The sensitivity of the sensor was determined to be 152.1 $mA\,cm^{-2}\,M^{-1}$ and the limit of detection (LOD, with S/N = 3) was 0.9 μM. The response time for steady-state current was 30–40 s. Interference of ascorbic acid (AA) and uric acid (UA) toward the detection of H_2O_2 was found to be negligible. Although the conditions of the photochemical reduction of AgNPs were not optimized, the low LOD (∼0.9 μM) in this study makes the AgNPs/ZnONRs/FTO electrode attractive for the determination of H_2O_2.

Acknowledgements

This work was sponsored by the National Research Council of Taiwan, the Republic of China, under grant number NSC 98-EC-17-A-02-S2-0125.

References

[1] M. Somasundrun, K. Kirtikara, M. Tanticharoen, Anal. Chim. Acta 319 (1996) 59–70.
[2] J. Wang, Y. Lin, L. Chen, Analyst 118 (1993) 227–280.
[3] M. Darder, K. Takada, F. Pariente, E. Lorenzo, H.D. Abruña, Anal. Chem. 71 (1999) 5530–5537.
[4] E.C. Hurdis, H. Romeyn, Anal. Chem. 26 (1954) 320–325.
[5] C. Matsubara, N. Kawamoto, K. Takamura, Analyst 117 (1992) 1781–1784.
[6] K. Nakashima, K. Maki, S. Kawaguchi, S. Akiyama, Y. Tsukamoto, K. Imai, Anal. Sci. 7 (1991) 709–719.
[7] M.E. Abbas, W. Luo, L. Zhu, J. Zou, H. Tang, Food Chem. 120 (2010) 327–331.
[8] A. Balamurugan, S.M. Chen, Electroanalysis 21 (2009) 1419–1423.
[9] L. Wang, E.K. Wang, Electrochem. Commun. 6 (2004) 225–229.
[10] J.S. Huang, D.W. Wang, H.Q. Hou, T.Y. You, Adv. Funct. Mater. 18 (2008) 441–448.
[11] M.R. Guascito, E. Filippo, C. Malitesta, D. Manno, A. Serra, A. Turco, Biosens. Bioelectron. 24 (2008) 1057–1063.
[12] B. Zho, Z. Liu, Z. Liu, G. Liu, Z. Li, J. Wang, X. Dong, Electrochem. Commun. 11 (2009) 1707–1710.
[13] Y. Song, K. Cui, L. Wang, S. Chen, Nanotechnology 20 (2009) 105501.
[14] K. Cui, Y. Song, Y. Yao, Z. Huang, L. Wang, Electrochem. Commun. 10 (2008) 663–667.
[15] C. Pacholski, A. Kornowski, H. Weller, Angew. Chem. Int. Ed. 43 (2004) 4774–4777.
[16] A. Wood, M. Giersig, P. Mulvaney, J. Phys. Chem. B 105 (2001) 8810–8815.
[17] A.L. Stroyuk, V.V. Shvalagin, S.Y. Kuchmii, J. Photochem. Photobiol. A 173 (2005) 185–194.
[18] V.V. Shvalagin, A.L. Stroyuk, S.Y. Kuchmii, J. Nanopart. Res. 9 (2007) 427–440.
[19] H. Hada, H. Tanemura, Y. Yonezawa, Bull. Chem. Soc. Jpn. 51 (1978) 3154–3160.
[20] R. Mishra, K. Rajanna, Sens. Mater. 17 (2005) 433–440.
[21] H. Koga, T. Kitaoka, H. Wariishi, J. Mater. Chem. 19 (2009) 2135–2140.
[22] M.J. Height, S.E. Prastinis, O. Mekasuwandumrong, P. Praserthdam, Appl. Catal. B 63 (2006) 305–312.
[23] S. Wu, H.T. Zhao, H.X. Ju, C.G. Shi, J.W. Zhao, Electrochem. Commun. 8 (2006) 1197–1203.
[24] C.M. Welch, C.E. Banks, A.O. Simm, R.G. Compton, Anal. Bioanal. Chem. 382 (2005) 12–21.
[25] A. Alivisatos, Science 271 (1996) 933–937.
[26] A.J Bard, L.R. Faulkner, Electrochemical Methods, Fundamentals and Applications, 2nd edition, John Wiley & Sons, New York, 2001.
[27] D.H. Lin, Y.X. Jiang, Y. Wang, S.G. Sun, J. Nanomater. 1 (2008) 473791.
[28] W. Lian, L. Wang, Y. Song, H. Yuan, S. Zhao, P. Li, L. Chen, Electrochim. Acta 54 (2009) 4334–4339.